JCTC Journal of Chemical Theory and Computation

Article

pubs.acs.org/JCTC

Assessing the Accuracy of Density Functional and Semiempirical Wave Function Methods for Water Nanoparticles: Comparing Binding and Relative Energies of $(H_2O)_{16}$ and $(H_2O)_{17}$ to CCSD(T) Results

Hannah R. Leverentz, Helena W. Qi,[†] and Donald G. Truhlar*

Department of Chemistry and Supercomputing Institute, University of Minnesota, Minneapolis, Minnesota 55455-0431, United States

Supporting Information

ABSTRACT: The binding energies and relative conformational energies of five configurations of the water 16-mer are computed using 61 levels of density functional (DF) theory, 12 methods combining DF theory with molecular mechanics damped dispersion (DF-MM), seven semiempirical-wave function (SWF) methods, and five methods combining SWF theory with molecular mechanics damped dispersion (SWF-MM). The accuracies of the computed energies are assessed by comparing them to recent high-level *ab initio* results; this assessment is more relevant to bulk water than previous tests on small clusters because a 16-mer is large enough to have water molecules that participate in more than three hydrogen bonds. We find that for water 16-mer binding energies the best DF, DF-MM, SWF, and SWF-MM methods (and their mean unsigned errors in kcal/mol) are respectively M06-2X (1.6), ωB97X-D (2.3), SCC-DFTB-γ^h (35.2), and PM3-D (3.2). We also mention the good performance of CAM-B3LYP (1.8), M05-2X (1.9), and TPSSLYP (3.0). In contrast, for relative energies of various water nanoparticle 16-mer structures, the best methods (and mean unsigned errors in kcal/mol), in the same order of classes of methods, are SOGGA11-X (0.3), ωB97X-D (0.2), PM6 (0.4), and PMOv1 (0.6). We also mention the good performance of LC-ωPBE-D3 (0.3) and ωB97X (0.4). When both relative and binding energies are taken into consideration, the best methods overall (out of the 85 tested) are M05-2X without molecular mechanics and ωB97X-D when molecular mechanics corrections are included; with considerably higher average errors and considerably lower cost, the best SWF or SWF-MM method is PMOv1. We use six of the best methods for binding energies of the water 16-mers to calculate the binding energies of water hexamers and water 17-mers to test whether these methods are also reliable for binding energy calculations on other types of water clusters.

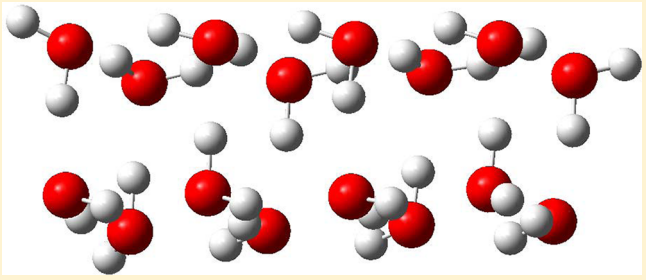

1. INTRODUCTION

Water in its various phases is, more than ever, a highly active area of both experimental and computational research.[1] Computational simulations using electronic structure theory are an ideal way to obtain detailed information about the multitude of hydrogen bond networks and proton transfer reactions that occur in the condensed phases of water. However, a myriad of electronic structure methods exist in varying degrees of both accuracy and computational cost, and often it can be difficult to know which level of electronic structure theory is the best one to use for a specific problem.

Highly correlated levels of wave function theory (WFT), such as coupled cluster theory with quasiperturbative triple excitations [CCSD(T)],[2−4] have been tested repeatedly against experimental data and consistently have been found to be reliable for the prediction of properties of a wide variety of systems. The drawback is that these methods are computationally demanding, and it would not be reasonable (or, in many cases, *possible*) to use them in large-scale simulations. Fortunately, the advent of density functional (DF) theory[5] has enabled electronic structure calculations to be performed on systems containing hundreds and even thousands of atoms. Semiempirical wave function (SWF) methods[6] are another possible avenue for investigating the electronic structures of even larger systems of water molecules, and they afford an orders of magnitude reduction in computing times. However, one still must be careful when selecting a DF or SWF method to use for a specific problem or a specific system: often a DF or SWF method that predicts certain properties, such as geometries or binding energies, will prove to be much less accurate for the computation of other properties, such as barrier heights or conformational energy differences. Therefore, before selecting a method to use for a specific problem, it is useful to test a variety of methods against experimental values or benchmark-quality computational results on similar systems.

Received: October 1, 2012
Published: December 11, 2012

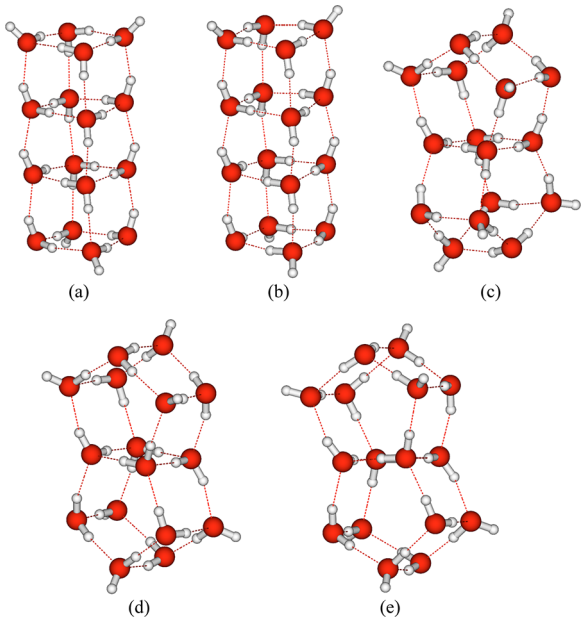

Figure 1. Water 16-mers from ref 32. The structures are (a) 4444-a, (b) 4444-b, (c) antiboat, (d) boat-a, and (e) boat-b.

The literature already contains a number of assessments of the accuracy of DF theory and SWF methods against high-level *ab initio* calculations for the prediction of binding energies and relative conformational energies of water clusters. For example, in 2005, Dahlke and Truhlar[7] computed the binding energies of 28 water dimers and eight water trimers at the Wiezmann-1[8,9] level of theory and used these as benchmarks to test the accuracy of 25 density functionals. They found that the PBE1W[7] functional had the lowest overall mean unsigned error (MUE)in the dimer and trimer binding energies, followed by the PW6B95,[10] B98,[11] and MPWB1K[12] functionals. In 2007, Olson et al.[13] computed the relative binding energies of six water hexamers at CCSD(T)/jul-cc-pVTZ,[14] and in 2008, Dahlke et al.[15] tested 11 density functionals against these benchmark calculations. They found that the PWB6K[10] functional had the lowest MUE over the relative energies of the six water hexamers in the MP2[16]/jul-cc-pVTZ optimized geometries (where jul-cc-pVTZ[14] is the cc-pVTZ[17−21] basis set on hydrogen atoms and the aug-cc-pVTZ[22,23] basis set on all heavy atoms; this was sometimes called aug′-cc-pVTZ or haTZ in older papers), followed by the MPWB1K, M05-2X,[24] PBE,[25] and PBE0[26] functionals. In 2012, Nachimuthu et al.[27] tested 15 density functionals and nine SWF methods for their ability to accurately predict energy differences between the products, reactants, and transition states of three different proton transfer reactions, including proton transfer in an $(H_5O_2)^+$ system. Over the energy differences associated with the proton transfer process in $(H_5O_2)^+$, Nachimuthu et al. found that the M06[28] and PW6B95 density functionals yielded the most accurate results and that SCC-DFTB[29] and PMOv1[30] were the most accurate of the SWF methods.

Until a short time ago, water hexamers were the largest water clusters on which CCSD(T) calculations with a triple-ζ or larger basis set had been performed.[31,32] To the best of our knowledge, levels of electronic structure theory even more accurate than CCSD(T), such as Weizmann-1, have never been used on clusters of that size. Recently, however, Yoo et al.[32] calculated the relative conformational energies of five water nanoparrticles, in particular water 16-mers, at the CCSD(T) level of electronic structure theory with the aug-cc-pVTZ basis set. Although water hexamers are an excellent test case for various electronic structure methods because they contain several two- and three-dimensional configurations within ∼1 kcal/mol of each other, none of the most stable water hexamers contains a four-coordinated water molecule, that is, a water molecule that participates in four hydrogen bonds like most water molecules in the interior of bulk water. The water nanoparticle 16-mers do contain four-coordinated water molecules. Therefore, updating our assessments of DF methods for water by testing them against these new benchmark calculations is very relevant to determining the best methods to use for water simulations. In this work, we test 73 DF methods[7,10−12,24−26,28,33−79] and 12 SWF methods[29,30,80−88] for their ability to accurately compute the relative energies and binding energies of the five water 16-mers against the corresponding CCSD(T)/aug-cc-pVTZ energies presented by Yoo et al. in ref 32. The CCSD(T)/aug-cc-pVTZ energies are not the definitive "last word" on the correct relative energies of these nanoparticles, but to date these are the highest-level *ab initio* calculations that have been performed on water nanoparticles this large, so we use these values are our current best

Table 1. Largest Internuclear Distance (Å) in Each Structure

structure name	structure type	atom 1[a]	atom 2[a]	distance
bag	$(H_2O)_6$	H(16)	H(18)	6.03
boat-1	$(H_2O)_6$	H(17)	H(18)	7.03
boat-2	$(H_2O)_6$	H(3)	H(11)	6.97
book-1	$(H_2O)_6$	H(12)	H(15)	6.79
book-2	$(H_2O)_6$	H(7)	H(13)	7.14
cage	$(H_2O)_6$	H(15)	H(18)	7.02
chair	$(H_2O)_6$	H(2)	H(12)	6.73
prism	$(H_2O)_6$	H(6)	H(18)	5.95
4444-a	$(H_2O)_{16}$	H(26)	H(32)	10.76
4444-b	$(H_2O)_{16}$	H(21)	H(23)	10.75
4444-b	$(H_2O)_{16}$	H(27)	H(39)	10.75[b]
antiboat	$(H_2O)_{16}$	H(32)	H(38)	10.21
boat-a	$(H_2O)_{16}$	H(5)	H(12)	10.63
boat-b	$(H_2O)_{16}$	H(41)	H(45)	10.63
sphere	$(H_2O)_{17}$	H(6)	H(14)	9.88
552′5	$(H_2O)_{17}$	H(24)	H(39)	9.35

[a]The largest internuclear distance in the given structure occurs between the two atoms described in these columns. The element symbol is followed by a number in parentheses that corresponds to its place in the list of coordinates for the given structure as it appears in the Supporting Information of this work. [b]The distance between atoms 27 and 39 of the 4444-b structure is exactly the same as the distance between atoms 21 and 23 of the 4444-b structure.

Table 2. Semiempirical Methods

semiempirical method	type	reference(s)
AM1	NDDO	82
AM1-D	NDDO/MM	80−82
MNDO	NDDO	83
PM3	NDDO	84
PM3-D	NDDO/MM	81, 82, 84
PM6	NDDO	85
PMOv1	NDDO/MM	30
RM1	NDDO	83
SCC-DFTB	SCTB	29
SCC-DFTB-γ^h	SCTB	29, 87
SCC-DFTB-D(LJ)	SCTB/MM	29, 88
SCC-DFTB-γ^h-D(LJ)	SCTB/MM	29, 87, 88

Table 3. Density Functionals

DFT name	type	references
BB95	meta-GGA	33, 34
BLYP	GGA	33, 35
BMK	hybrid meta-GGA	36
B1B95	hybrid meta-GGA	33, 34
B3LYP	hybrid GGA	34, 35, 37
B97-1	hybrid GGA	38
B97-2	hybrid GGA	39
B97-3	hybrid GGA	40
B97-D	GGA/MM	41
B97-D3[a]	GGA/MM	41, 42
B97-D3(BJ)[a]	GGA/MM	41−45
B98	hybrid GGA	11
CAM-B3LYP	hybrid GGA	46
GKSVWN5[b]	LSDA	47, 48
HCTH	GGA	38
HSE06[c]	hybrid GGA	49
LC-ωPBE	hybrid GGA	50
LC-ωPBE-D3[a]	hybrid GGA/MM	42, 50
LC-ωPBE-D3(BJ)[a]	hybrid GGA/MM	42−45, 50
MN12-L	meta-NGA	51
MN12-SX	hybrid meta-NGA	52
MPW1B95	hybrid meta-GGA	12, 34, 53
MPW1B95-D3[a]	hybrid meta-GGA/MM	12, 34, 42, 53
MPW1B95-D3(BJ)[a]	hybrid meta-GGA/MM	12, 34, 42−45, 53
MPW1K	hybrid GGA	53−55
MPW1LYP	hybrid GGA	35, 53
MPW1PBE	hybrid GGA	25, 53
*m*PW1PW[d]	hybrid GGA	53, 54
MPW3LYP	hybrid GGA	35, 53
MPW3PBE	hybrid GGA	25, 53
MPWB1K	hybrid meta-GGA	12, 34, 53
MPWKCIS1K	hybrid meta-GGA	56
*m*PWLYP	GGA	35, 53
MPWLYP1W	GGA	7
M05	hybrid meta-GGA	57
M05-2X	hybrid meta-GGA	24
M06	hybrid meta-GGA	28
M06-2X	hybrid meta-GGA	28
M06-L	meta-GGA	58
M08-HX	hybrid meta-GGA	59
M08-SO	hybrid meta-GGA	59
M11	hybrid meta-GGA	60
M11-L	meta-GGA	61
N12	NGA	62
N12-SX	hybrid NGA	52
OLYP	GGA	35, 63, 64
OptX[e]	GGA	63, 64
O3LYP	hybrid GGA	65
PBE	GGA	25
PBE0[f]	hybrid GGA	26
PBE1KCIS	hybrid meta-GGA	25, 66−69
PBE1W	GGA	7
PBELYP	GGA	25, 35
PBELYP1W	GGA	7
PBEX[e]	GGA	25
PW6B95	hybrid meta-GGA	10, 34, 53
PW6B95-D3[a]	hybrid meta-GGA/MM	10, 34, 42, 53
PW6B95-D3(BJ)[a]	hybrid meta-GGA/MM	10, 34, 42−45, 53
PWB6K	hybrid meta-GGA	10, 34, 53
revPBE	GGA	70
revPBE-D3[a]	GGA/MM	42, 70
revPBE-D3(BJ)[a]	GGA/MM	42−45, 70
revTPSS	meta-GGA	71
SOGGA11-X	hybrid GGA	72
TPSS	meta-GGA	73, 74
TPSSh	hybrid meta-GGA	75
TPSSLYP	meta-GGA	35, 73, 74
TPSSLYP1W	meta-GGA	7
X3LYP	hybrid GGA	33, 35, 53, 76
τHCTHhyb	hybrid meta-GGA	77
ωB97	hybrid GGA	78
ωB97X	hybrid GGA	78
ωB97X-D	hybrid GGA/MM	79

[a]D3 means that the damping function proposed by Grimme in ref 42 is being used in the calculation of the D3 dispersion energy, and D3(BJ) means that the damping function proposed by Becke and Johnson in refs 43−45 is being used in the calculation of the D3 dispersion energy. Note that D3 damps the dispersion term to zero at the origin, whereas D3(BJ) damps it to a finite value. [b]The *Gaussian* keyword for this functional is SVWN5. [c]Also called HSE, but not to be confused with the original HSE of 2003. The *Gaussian* keyword for this functional is HSEh1PBE. [d]Also called *m*PW0. [e]Exchange only (no correlation). [f]The *Gaussian* keyword for this functional is PBE1PBE. This functional is also sometimes referred to as PBEh.

estimates. Of the DF methods, 61 are electronic structure calculations without post-SCF corrections (straight DF), and 12 are combinations of electronic structure theory with molecular mechanics (DF-MM). Of the SWF methods, the same division gives seven straight SWF and five SWF-MM.

After using the binding and relative energies of the water 16-mers to test which are the best DF, DF-MM, SWF, SWF-MM methods for water nanoparticle 16-mers, we apply six of the better performing methods to water hexamers and water 17-mers to test whether these methods are capable of yielding accurate binding energies for water clusters of other sizes as well.

2. METHODS AND SOFTWARE

The geometries of the five water 16-mers and the two water 17-mers used in this study are the MP2/aug-cc-pVTZ optimized geometries taken from the Supporting Information of ref 32. The five water 16-mers are shown in Figure 1, and the two water 17-mers are shown in Figure 3. Table 1 gives an idea of the size of each structure used in this study by listing the largest internuclear distance that occurs in each one. One can see that each of the water 16-mers contains at least one internuclear distance greater than 10 Å and may therefore be classified as a nanoparticle. In order to calculate the binding energies of these clusters and nanoparticles, the energy of a water monomer is needed but is not provided in the Supporting Information of ref 32. Therefore, a geometry optimization of a gas-phase water molecule was performed using MP2 with the aug-cc-pVTZ basis set. We calculated a single-point CCSD(T)/aug-cc-pVTZ electronic plus nuclear repulsion energy of the water molecule at the MP2/aug-cc-pVTZ optimized geometry to obtain the 16-mer and 17-mer benchmark binding energies presented in this work, and we calculated the single-point monomer energy with each of the 85 methods tested in order to get the

Table 4. Binding Energies (kcal/mol) of Water 16-mers and Mean Unsigned Errors (MUE, kcal/mol) in NDDO, NDDO/MM, and SCTB Calculations

method	4444-a	4444-b	antiboat	boat-a	boat-b	MSE	MUE
CCSD(T)/aug-cc-pVTZ	171.06	170.52	170.55	170.80	170.64	0.0	0.0
PM3-D	175.08	175.83	174.21	172.53	172.05	3.2	3.2
PMOv1	156.33	156.53	157.12	157.11	157.20	−13.9	13.9
AM1-D	167.82	167.23	147.64	146.63	146.81	−15.5	15.5
SCC-DFTB-γ^h	137.07	137.07	134.75	134.32	134.18	−35.2	35.2
PM6	118.05	118.10	117.89	118.60	118.51	−52.5	52.5
SCC-DFTB-γ^h-D(LJ)	117.64	117.14	116.29	114.97	114.87	−54.5	54.5
SCC-DFTB	104.03	103.62	102.41	101.76	101.66	−68.0	68.0
PM3	92.18	91.68	95.20	93.52	93.14	−77.6	77.6
SCC-DFTB-D(LJ)	84.59	83.70	83.96	82.40	82.35	−87.3	87.3
AM1	52.85	50.10	37.20	35.99	36.39	−128.2	128.2
RM1	24.62	24.58	34.36	31.92	31.89	−141.2	141.2
MNDO	−292.97	−299.94	−282.49	−286.84	−286.48	−460.5	460.5

binding energies for those methods. Note that the tests of relative binding energies are independent of the monomer energies, but the tests for absolute binding energies do require these monomer energies. In the Supporting Information of this work, we present the binding energies and characteristic errors (which will be defined later) of the water 16-mers and 17-mers that are obtained when the M06-L[58]/aug-cc-pVTZ optimized water monomer geometry is used to show that the conclusions drawn in this work do not depend strongly on the particular water monomer geometry used to obtain the binding energies.

The geometries of the eight water hexamers used in this study are the MP2/jul-cc-pVTZ optimized structures taken from the Supporting Information of ref 31 (note that the jul-cc-pVTZ basis set is exactly the same as the "haTZ" basis set described in ref 31). The Supporting Information of ref 31 also provides the MP2/jul-cc-pVTZ optimized gas-phase geometry of the water monomer, and all water hexamer binding energies reported in this work are taken relative to six infinitely separated water monomers in the MP2/jul-cc-pVTZ optimized gas-phase geometry at the given level of theory.

Single-point energy calculations were performed on the five water 16-mers and the MP2 optimized water molecule with the 12 SWF methods given in Table 2 and with the 71 DF methods given in Table 3. The jun-cc-pVTZ[14] basis set was used for all DF calculations. All SWF calculations were done using a modified version of MOPAC 5.018mn[89] (in particular, MOPAC 5.019mn-alpha3). All DF calculations were performed using the *Minnesota Gaussian Functional Module* (MN-GFM), version 6.4,[90] which is a locally modified version of the *Gaussian 09* electronic structure package, revision c01.[91] For all DF calculations, the *Gaussian* keyword "integral=(grid=ultrafine)" was used. In order to compute the D3 and D3(BJ) dispersion energies of Grimme and co-workers[42] that is used in some of the density functionals (*vide infra*), the *DFT-D3*, version 2.1, revision 3[92] software was used. The reader should note that the dispersion energy corrections (of both the -D and -D3 methods) contain different parameters for different density functionals; for example, the D3 energy correction for the LC-ωPBE functional is not the same as that for the B97 functional. For the SCC-DFTB,[29] SCC-DFTB-γ^h,[29,87] SCC-DFTB-D(LJ),[29,88] and SCC-DFTB-γ^h-D(LJ)[29,87,88] calculations (which will be described in greater detail below), the *DFTB+* version 1.2 program package[93] was used with the mio-1-1[94] Slater-Koster[95] files.

3. RESULTS AND DISCUSSION

Before discussing the results, we introduce the methods to be tested. They fall into 15 broad categories of approximation methods, all of which involve self-consistent field (SCF) calculations. Some involve WF theory, and others involve DF theory:

1. Neglect of diatomic differential overlap approximations (NDDO). This is a popular version of SWF theory, and it is represented by five examples in Table 2.

2. NDDO plus molecular mechanics terms (NDDO/MM). Analytic damped dispersion approximations are added to an NDDO calculation. There are three examples in Table 2.

3. Self-consistent tight-binding (SCTB) method. This class of methods also goes under other names, such as ω technique in the Hückel method[96] and iterative extended Hückel theory.[97] There are two examples from this category in Table 2: SCC-DFTB[29] and SCC-DFTB-γ^h.[29,87] Here, we use SCC-DFTB to mean its original formulation in ref 29; for clarity, we note that this is the same as the method referred to as DFTB2 in ref 98. We use the term SCC-DFTB-γ^h to mean the method that is called DFTB2-γ^h in ref 98. This is the same as the original SCC-DFTB method except that it contains an exponential damping factor in the term that describes the interaction between a charge on a hydrogen atom and a charge on a heavy atom.[87]

4. SCTB plus molecular mechanics terms (SCTB/MM). Analytic damped dispersion approximations are added to an SCTB calculation. There are two examples in Table 2: SCC-DFTB-D(LJ) and SCC-DFTB-γ^h-D(LJ). The "-D(LJ)" means that a Lennard-Jones dispersion potential[88] with the Universal Force Field (UFF)[99] parameters was added to the energy expressions in the SCC-DFTB and SCC-DFTB-γ^h methods.

5. Local spin density approximation (LSDA). This is the simplest form of DFT, sometimes called the local density approximation (LDA) when only closed-shell systems are considered. Here we use one of the oldest versions, GKSVWN5 (Table 3), in which the parameters are based on the uniform-electron-gas model.

6. Generalized gradient approximation (GGA). In this form of density functional, the exchange-correlation energy (E_{xc}) is written as the sum of an exchange term that is a product of a function of the spin densities and a function of the spin-labeled reduced density gradients and a correlation term that also depends on these quantities. There are 12 examples in Table 3.

7. Nonseparable gradient approximation (NGA). This form of density functional is the same as a GGA except that the separable exchange term of a GGA is replaced by a

Table 5. Binding Energies (kcal/mol) of Water 16-mers and Mean Unsigned Errors (MUE, kcal/mol) in Density Functional Calculations

method	4444-a	4444-b	antiboat	boat-a	boat-b	MSE	MUE
CCSD(T)/aug-cc-pVTZ	171.06	170.52	170.55	170.80	170.64	0.0	0.0
			LSDA				
GKSVWN5	269.58	270.45	269.28	270.57	270.21	99.3	99.3
			GGA and NGA				
PBE	162.67	162.24	166.10	166.67	166.46	−5.9	5.9
PBELYP	177.84	177.09	180.49	180.94	180.70	8.7	8.7
*m*PWLYP	157.73	156.96	161.41	161.86	161.63	−10.8	10.8
PBE1W	151.89	151.23	155.70	156.15	155.95	−16.5	16.5
PBELYP1W	151.13	150.13	154.80	155.09	154.89	−17.5	17.5
MPWLYP1W	150.75	149.92	154.72	155.12	154.91	−17.6	17.6
N12	147.14	146.90	151.78	152.36	152.11	−20.7	20.7
BLYP	133.69	132.87	138.02	138.43	138.23	−34.5	34.5
HCTH	115.93	114.65	122.44	122.42	122.26	−51.2	51.2
revPBE	109.48	108.53	115.33	115.63	115.46	−57.8	57.8
PBEX	83.62	81.75	89.60	89.51	89.39	−83.9	83.9
OLYP	69.52	68.13	77.96	77.98	77.83	−96.4	96.4
OptX	−21.81	−24.32	−10.41	−10.92	−10.96	−186.4	186.4
			GGA/MM				
revPBE-D3	155.65	155.05	156.40	156.48	156.33	−14.7	14.7
revPBE-D3(BJ)	152.56	151.97	154.09	154.49	154.29	−17.2	17.2
B97-D	152.58	152.17	153.19	153.98	153.79	−17.6	17.6
B97-D3(BJ)	199.45	199.45	195.39	196.31	196.08	26.6	26.6
B97-D3	201.47	201.43	196.62	197.31	197.11	28.1	28.1
			meta-GGA and meta-NGA				
TPSSLYP	165.38	164.69	169.25	169.67	169.43	−3.0	3.0
M06-L	164.52	164.20	160.79	161.24	161.13	−8.3	8.3
TPSSLYP1W	150.21	149.37	154.67	154.99	154.78	−17.9	17.9
revTPSS	147.59	147.06	150.73	151.20	151.04	−21.2	21.2
TPSS	145.58	145.10	150.50	150.98	150.78	−22.1	22.1
M11-L	144.90	144.42	142.37	142.61	142.47	−27.4	27.4
MN12-L	138.86	138.32	134.29	134.99	134.93	−34.4	34.4
BB95	117.87	117.24	121.31	121.82	121.67	−50.7	50.7
			hybrid GGA and hybrid NGA				
CAM-B3LYP	167.70	167.24	169.63	170.09	169.89	−1.8	1.8
N12-SX	166.22	165.81	167.84	168.32	168.13	−3.5	3.5
MPW3LYP	162.26	161.62	165.08	165.47	165.28	−6.8	6.8
HSE06	161.70	161.32	164.52	165.00	164.82	−7.2	7.2
MPW1LYP	159.72	159.01	162.37	162.71	162.52	−9.4	9.4
ωB97X	181.23	180.79	180.06	180.44	180.30	9.9	9.9
PBE0	158.17	157.76	161.00	161.46	161.28	−10.8	10.8
X3LYP	155.70	155.06	158.57	158.96	158.77	−13.3	13.3
ωB97	186.00	185.59	183.16	183.58	183.45	13.6	13.6
B97−1	154.87	154.20	157.28	157.61	157.45	−14.4	14.4
SOGGA11-X	153.95	153.53	152.98	153.48	153.36	−17.3	17.3
B98	149.07	148.40	152.04	152.37	152.21	−19.9	19.9
MPW3PBE	147.84	147.40	151.60	152.08	151.90	−20.5	20.5
MPW1K	146.02	145.59	149.08	149.46	149.30	−22.8	22.8
B3LYP	144.59	143.90	147.90	148.26	148.08	−24.2	24.2
*m*PW1PW	144.13	143.67	147.80	148.25	148.07	−24.3	24.3
MPW1PBE	143.02	142.58	146.84	147.30	147.12	−25.3	25.3
LC-ωPBE	142.18	141.66	144.60	144.98	144.84	−27.1	27.1
B97−3	132.28	131.39	134.15	134.35	134.23	−37.4	37.4
B97−2	124.43	123.70	128.74	129.00	128.86	−43.8	43.8
O3LYP	88.10	86.89	95.20	95.26	95.12	−78.6	78.6
			hybrid GGA/MM				
ωB97X-D	168.76	168.42	168.12	168.41	168.26	−2.3	2.3
LC-ωPBE-D3	166.63	166.25	166.72	166.95	166.80	−4.0	4.0
LC-ωPBE-D3(BJ)	161.02	160.61	161.78	162.16	162.00	−9.2	9.2

dx.doi.org/10.1021/ct300848z | J. Chem. Theory Comput. 2013, 9, 995−1006

Table 5. continued

method	4444-a	4444-b	antiboat	boat-a	boat-b	MSE	MUE
hybrid meta-GGA and hybrid meta-NGA							
M06-2X	172.05	171.82	168.33	169.12	169.01	−0.6	1.6
M05-2X	169.74	169.34	167.95	168.57	168.47	−1.9	1.9
M08-HX	167.51	167.00	164.75	165.43	165.34	−4.7	4.7
M08-SO	165.04	164.45	161.74	162.25	162.17	−7.6	7.6
M06	166.14	165.85	160.05	160.60	160.52	−8.1	8.1
M11	161.62	161.30	158.43	159.18	159.08	−10.8	10.8
M05	159.53	158.70	160.15	160.24	160.11	−11.0	11.0
PBE1KCIS	153.69	153.06	156.68	157.05	156.87	−15.2	15.2
τHCTHhyb	150.65	150.25	154.00	154.48	154.29	−18.0	18.0
BMK	150.33	149.88	147.51	148.12	148.03	−21.9	21.9
MN12-SX	149.89	149.20	146.81	147.33	147.21	−22.6	22.6
TPSSh	144.78	144.30	149.33	149.76	149.57	−23.2	23.2
PW6B95	145.70	145.06	147.31	147.67	147.54	−24.1	24.1
PWB6K	145.70	145.19	147.01	147.36	147.25	−24.2	24.2
MPWB1K	145.36	144.84	146.73	147.09	146.98	−24.5	24.5
MPW1B95	143.50	142.96	145.29	145.70	145.57	−26.1	26.1
MPWKCIS1K	140.19	139.57	143.42	143.70	143.56	−28.6	28.6
B1B95	125.23	124.63	127.67	128.05	127.94	−44.0	44.0
hybrid meta-GGA/MM							
MPW1B95-D3	160.80	160.38	161.18	161.47	161.36	−9.7	9.7
PW6B95-D3	160.66	160.13	161.18	161.44	161.33	−9.8	9.8
PW6B95-D3(BJ)	156.01	155.42	156.90	157.25	157.11	−14.2	14.2
MPW1B95-D3(BJ)	154.67	154.18	155.66	156.06	155.91	−15.4	15.4

nonseparable exchange-correlation term. There is one example in Table 3.

8. GGA plus molecular mechanics terms (GGA/MM). Analytic damped dispersion approximations are added to a GGA calculation. There are three examples in Table 3.

9. Hybrid GGA. Some portion of the exchange energy of a GGA functional is calculated by the Hartree−Fock expression. There are 20 examples in Table 3.

10. Hybrid NGA. Some portion of the exchange energy of a NGA functional is calculated by the Hartree−Fock expression. There is one example in Table 3.

11. Hybrid GGA/MM. Some portion of the exchange energy of a GGA/MM functional is calculated by the Hartree−Fock expression. There are three examples in Table 3.

12. Meta nonseparable gradient approximation (meta-NGA). In this extension of the NGA form, E_{xc} also depends on the spin-labeled kinetic energy densities. There is one example in Table 3.

13. Hybrid meta-GGA. Some portion of the exchange energy of a meta-GGA functional is calculated by the Hartree−Fock expression. There are 16 examples in Table 3.

14. Hybrid meta-NGA. Some portion of the exchange energy of a meta-NGA functional is calculated by the Hartree−Fock expression. There is one example in Table 3.

15. Hybrid meta-GGA plus molecular mechanics terms (hybrid meta-GGA/MM). Analytic damped dispersion approximations are added to a hybrid meta-GGA density functional. There are two examples in Table 3.

Tables 4 and 5 show the binding energies of the water 16-mers calculated at various levels of semiempirical molecular orbital theory and with several density functionals, respectively. Binding energies are important because if a method cannot predict an accurate binding energy, then that method cannot be trusted to predict correct vapor pressures, heats of vaporization, boiling points, etc. The binding energy (E_{bind}) of a water 16-mer for method X is calculated as

$$E_{bind} = 16E^{X}_{H_2O} - E^{X}_{Y} \quad (1)$$

where $E^{X}_{H_2O}$ is the single-point energy of the water monomer in its MP2/aug-cc-pVTZ optimized gas-phase geometry at level X and where E^{X}_{Y} is the single-point energy of nanoparticle Y in its MP2/aug-cc-pVTZ optimized geometry (taken from the Supporting Information of ref 32) at level X. These tables also contain the mean signed errors (MSE) and mean unsigned errors (MUE) where the errors are calculated relative to the CCSD(T)/aug-cc-pVTZ binding energies. To calculate the CCSD(T)/aug-cc-pVTZ binding energies, we used the total electronic plus nuclear repulsion energies of the nanoparticles

Table 6. Relative Energies (kcal/mol) of Water 16-mers and Mean Unsigned Errors (MUE, kcal/mol) in NDDO, NDDO/MM, and SCTB Calculations

method	4444-a	4444-b	antiboat	boat-a	boat-b	MUE[a]
CCSD(T)/aug-cc-pVTZ	0.00	0.54	0.51	0.25	0.42	0.0
PM6	0.00	−0.05	0.16	−0.55	−0.46	0.4
PMOv1	0.00	−0.20	−0.79	−0.78	−0.87	0.6
SCC-DFTB-D(LJ)	0.00	0.90	0.64	2.19	2.24	1.1
SCC-DFTB	0.00	0.41	1.61	2.27	2.36	1.2
SCC-DFTB-γ^h-D(LJ)	0.00	0.49	1.35	2.67	2.77	1.5
SCC-DFTB-γ^h	0.00	0.00	2.32	2.75	2.90	1.7
PM3	0.00	0.50	−3.02	−1.34	−0.96	1.7
PM3-D	0.00	−0.75	0.87	2.55	3.03	2.0
RM1	0.00	0.04	−9.74	−7.30	−7.27	5.5
MNDO	0.00	6.97	−10.48	−6.13	−6.49	8.3
AM1	0.00	2.75	15.65	16.86	16.46	9.4
AM1-D	0.00	0.59	20.18	21.19	21.01	12.5

[a]The mean unsigned error is taken over the 10 energy differences that exist between all possible pairs of the five water 16-mer configurations.

dx.doi.org/10.1021/ct300848z | J. Chem. Theory Comput. 2013, 9, 995−1006

Table 7. Relative Energies (kcal/mol) of Water 16-mers and Mean Unsigned Errors (MUE, kcal/mol) in Density Functional Calculations

method	4444-a	4444-b	antiboat	boat-a	boat-b	MUE[a]
CCSD(T)/aug-cc-pVTZ	0.00	0.54	0.51	0.25	0.42	0.0
LSDA						
GKSVWN5	0.00	−0.88	0.30	−0.99	−0.63	0.8
GGA and NGA						
PBELYP	0.00	0.75	−2.65	−3.10	−2.86	2.1
PBE	0.00	0.43	−3.43	−4.00	−3.79	2.5
PBELYP1W	0.00	1.00	−3.68	−3.97	−3.77	2.7
*m*PWLYP	0.00	0.76	−3.69	−4.13	−3.91	2.7
PBE1W	0.00	0.67	−3.81	−4.26	−4.06	2.8
MPWLYP1W	0.00	0.83	−3.97	−4.37	−4.16	2.9
BLYP	0.00	0.82	−4.33	−4.74	−4.54	3.1
N12	0.00	0.24	−4.63	−5.21	−4.97	3.2
revPBE	0.00	0.95	−5.85	−6.15	−5.98	4.0
PBEX	0.00	1.88	−5.98	−5.89	−5.77	4.4
HCTH	0.00	1.27	−6.51	−6.49	−6.33	4.5
OLYP	0.00	1.39	−8.43	−8.46	−8.31	5.7
OptX	0.00	2.51	−11.40	−10.89	−10.85	7.8
GGA/MM						
revPBE-D3	0.00	0.59	−0.75	−0.83	−0.68	0.7
B97-D	0.00	0.41	−0.61	−1.40	−1.21	1.0
revPBE-D3(BJ)	0.00	0.59	−1.53	−1.93	−1.73	1.3
B97-D3(BJ)	0.00	0.00	4.06	3.14	3.37	2.2
B97-D3	0.00	0.03	4.84	4.16	4.35	2.7
meta-GGA and meta-NGA						
M11-L	0.00	0.49	2.53	2.29	2.43	1.2
M06-L	0.00	0.32	3.73	3.28	3.38	2.0
revTPSS	0.00	0.53	−3.14	−3.62	−3.45	2.3
MN12-L	0.00	0.54	4.57	3.87	3.92	2.3
BB95	0.00	0.63	−3.44	−3.94	−3.80	2.6
TPSSLYP	0.00	0.69	−3.88	−4.29	−4.06	2.8
TPSSLYP1W	0.00	0.84	−4.47	−4.78	−4.57	3.1
TPSS	0.00	0.48	−4.92	−5.40	−5.19	3.4
hybrid GGA and hybrid NGA						
SOGGA11-X	0.00	0.42	0.97	0.47	0.60	0.3
*ω*B97X	0.00	0.45	1.17	0.80	0.93	0.4
N12-SX	0.00	0.41	−1.63	−2.10	−1.91	1.4
*ω*B97	0.00	0.41	2.85	2.42	2.55	1.4
CAM-B3LYP	0.00	0.46	−1.93	−2.39	−2.20	1.6
B97−3	0.00	0.89	−1.87	−2.07	−1.95	1.6
LC-*ω*PBE	0.00	0.51	−2.42	−2.80	−2.66	1.8
B97−1	0.00	0.68	−2.41	−2.74	−2.58	1.9
MPW1LYP	0.00	0.71	−2.65	−2.99	−2.80	2.0
HSE06	0.00	0.38	−2.82	−3.30	−3.12	2.1
PBE0	0.00	0.42	−2.83	−3.29	−3.11	2.1
MPW3LYP	0.00	0.64	−2.82	−3.21	−3.01	2.1
X3LYP	0.00	0.64	−2.87	−3.26	−3.07	2.1
B98	0.00	0.67	−2.97	−3.30	−3.14	2.2
MPW1K	0.00	0.43	−3.06	−3.44	−3.28	2.2
B3LYP	0.00	0.69	−3.31	−3.67	−3.49	2.4
*m*PW1PW	0.00	0.46	−3.68	−4.12	−3.95	2.6
MPW3PBE	0.00	0.44	−3.76	−4.24	−4.06	2.7
MPW1PBE	0.00	0.44	−3.82	−4.27	−4.10	2.7
B97−2	0.00	0.73	−4.31	−4.58	−4.43	3.0
O3LYP	0.00	1.21	−7.10	−7.16	−7.02	4.8
hybrid GGA/MM						
*ω*B97X-D	0.00	0.34	0.64	0.35	0.50	0.2
LC-*ω*PBE-D3	0.00	0.38	−0.09	−0.32	−0.17	0.3
LC-*ω*PBE-D3(BJ)	0.00	0.41	−0.76	−1.14	−0.98	0.8

dx.doi.org/10.1021/ct300848z | J. Chem. Theory Comput. 2013, 9, 995−1006

Table 7. continued

method	4444-a	4444-b	antiboat	boat-a	boat-b	MUE[a]
			hybrid meta-GGA and hybrid meta-NGA			
M05-2X	0.00	0.41	1.79	1.17	1.27	0.8
M05	0.00	0.83	−0.62	−0.71	−0.59	0.8
PWB6K	0.00	0.51	−1.31	−1.66	−1.55	1.2
MPWB1K	0.00	0.51	−1.37	−1.73	−1.62	1.2
M08-HX	0.00	0.50	2.76	2.07	2.17	1.3
BMK	0.00	0.45	2.83	2.22	2.31	1.4
PW6B95	0.00	0.63	−1.61	−1.97	−1.85	1.4
MN12-SX	0.00	0.70	3.09	2.57	2.69	1.5
MPW1B95	0.00	0.54	−1.79	−2.20	−2.07	1.5
M11	0.00	0.32	3.19	2.44	2.53	1.6
M08-SO	0.00	0.59	3.30	2.79	2.87	1.6
B1B95	0.00	0.60	−2.44	−2.82	−2.71	1.9
M06-2X	0.00	0.23	3.72	2.93	3.04	1.9
PBE1KCIS	0.00	0.63	−2.99	−3.36	−3.18	2.2
MPWKCIS1K	0.00	0.62	−3.22	−3.51	−3.37	2.3
τHCTHhyb	0.00	0.40	−3.35	−3.82	−3.64	2.4
TPSSh	0.00	0.48	−4.54	−4.98	−4.79	3.1
M06	0.00	0.28	6.09	5.53	5.62	3.4
			hybrid meta-GGA/MM			
MPW1B95-D3	0.00	0.41	−0.38	−0.67	−0.56	0.6
PW6B95-D3	0.00	0.53	−0.51	−0.78	−0.66	0.6
PW6B95-D3(BJ)	0.00	0.59	−0.89	−1.24	−1.10	0.9
MPW1B95-D3(BJ)	0.00	0.49	−0.99	−1.39	−1.25	1.0

[a]The mean unsigned error is taken over the 10 energy differences that exist between all possible pairs of the five water 16-mer configurations.

given in ref 32 as E_Y^X and we performed the $E_{H_2O}^X$ calculations ourselves using *Gaussian 09*.

The overall best method for capturing the binding energies of the water 16-mers is the hybrid meta-GGA density functional M06-2X, with an MUE of only 1.6 kcal/mol. Closely following in second place is the hybrid GGA density functional CAM-B3LYP, with an MUE in binding energies of only 1.8 kcal/mol. Hybrid functionals contain a portion of the "Hartree−Fock" exchange, which is a short name for the exchange energy computed from the approximate Kohn−Sham orbitals by the Hartree−Fock expression for the exchange energy of a single Slater determinant (The Kohn−Sham orbitals are approximate because we employ an approximate exchange−correlation energy functional; the Hartree−Fock exchange would be exact if one were to employ the exact density functional, which is unknown, and it would equal the exchange energy of Hartree−Fock theory if we were to employ the Hartree−Fock orbitals). This type of exchange is nonlocal; all functionals considered here that do not have Hartree−Fock exchange are local ("local" is more general than "local-density," the special case in which the functional depends only on densities). For large systems, nonlocal terms can increase the computational cost of an energy calculation considerably, so it is interesting to know which local functional does best, and we find that this is TPSSLYP, with an MUE of only 3.0 kcal/mol. Not far behind TPSSLYP is an NDDO/MM method, PM3-D, with an MUE of only 3.2 kcal/mol.

Tables 6 and 7 show the energy of each nanoparticle relative to the 4444-a structure at each level of SWF and DF theory. A method that does not predict relative energies correctly will have difficulty predicting the most stable geometries of a system of water molecules and at best can get them right by cancellation of errors. The 4444-a structure is the most stable of the water 16-mers according to the CCSD(T)/aug-cc-pVTZ calculations. Within a set of five structures, there are 10 possible pairs of structures and therefore 10 possible relative energies that can be determined. The mean signed and unsigned errors shown in Tables 6 and 7 are calculated with respect to the CCSD(T)/aug-cc-pVTZ values over all 10 possible energy differences. Predicting these 10 relative energies is an especially challenging test for all of these SWF and DF methods because all 10 energy differences are under 0.6 kcal/mol; these water 16-mer configurations are very close to one another in energy. The best methods for predicting these relative energies are all hybrid GGA or hybrid GGA/MM functionals: ωB97X-D (MUE = 0.2 kcal/mol), SOGGA11-X (MUE = 0.3 kcal/mol), and LC-ωPBE-D3 (MUE = 0.3 kcal/mol). The best nonhybrid density functional for predicting the relative energies is the GGA/MM functional revPBE-D3 with an MUE of 0.7 kcal/mol. Two SWF methods actually outperform all of the nonhybrid DFT methods for these relative energy calculations: PM6 (MUE = 0.4 kcal/mol) and PMOv1 (MUE = 0.6 kcal/mol).

Table 8 shows the characteristic error (CE) of each of the 85 methods studied for the 16-mers. The CE is computed as follows:

$$\mathrm{CE} = 0.5\left(\frac{\mathrm{MUE}_{\mathrm{BE}}^{X}}{\mathrm{MUE}_{\mathrm{BE}}^{\mathrm{med}}}\right) + 0.5\left(\frac{\mathrm{MUE}_{\mathrm{RE}}^{X}}{\mathrm{MUE}_{\mathrm{RE}}^{\mathrm{med}}}\right) \quad (2)$$

In eq 2, $\mathrm{MUE}_{\mathrm{BE}}^{X}$ is the mean unsigned error in the five binding energies calculated by method X and $\mathrm{MUE}_{\mathrm{RE}}^{X}$ is the mean unsigned error in the 10 relative energies calculated by method X. $\mathrm{MUE}_{\mathrm{BE}}^{\mathrm{med}}$ is 19.9 kcal/mol, which is the median of all of the $\mathrm{MUE}_{\mathrm{BE}}^{X}$ values for all 85 methods. $\mathrm{MUE}_{\mathrm{RE}}^{\mathrm{med}}$ is 2.0 kcal/mol, which is the median of all of the $\mathrm{MUE}_{\mathrm{BE}}^{X}$ values for all 85 methods. Defining the CE in this way enables us to put the errors in binding energies and relative energies on an equal footing and to pick out the "most likely to succeed" density functionals and SWF methods for water calculations in a quantitative way. Methods with a CE of 1.0 can be considered to be

Table 8. Characteristic Errors[a] (CE) in Semiempirical and Density Functional Methods for 16-mers

method	method type	CE[a]
ωB97X-D	hybrid GGA/MM	0.10
LC-ωPBE-D3	hybrid GGA/MM	0.18
M05-2X	hybrid meta-GGA	0.23
ωB97X	hybrid GGA	0.35
MPW1B95-D3	hybrid meta-GGA/MM	0.38
PW6B95-D3	hybrid meta-GGA/MM	0.40
N12-SX	hybrid NGA	0.43
LC-ωPBE-D3(BJ)	hybrid GGA/MM	0.43
CAM-B3LYP	hybrid GGA	0.43
M08-HX	hybrid meta-GGA	0.44
M05	hybrid meta-GGA	0.47
SOGGA11-X	hybrid GGA	0.50
PMOv1	NDDO/MM	0.50
M06-2X	hybrid meta-GGA	0.52
revPBE-D3	GGA/MM	0.55
PM3-D	NDDO/MM	0.58
PW6B95-D3(BJ)	hybrid meta-GGA/MM	0.59
M08-SO	hybrid meta-GGA	0.59
MPW1B95-D3(BJ)	hybrid meta-GGA/MM	0.63
M11	hybrid meta-GGA	0.67
B97-D	GGA/MM	0.68
MPW3LYP	hybrid GGA	0.69
ωB97	hybrid GGA	0.69
M06-L	meta-GGA	0.70
HSE06	hybrid GGA	0.70
PBELYP	GGA	0.73
MPW1LYP	hybrid GGA	0.73
revPBE-D3(BJ)	GGA/MM	0.76
TPSSLYP	meta-GGA	0.76
PBE	GGA	0.77
PBE0	hybrid GGA	0.79
B97−1	hybrid GGA	0.82
X3LYP	hybrid GGA	0.86
BMK	hybrid meta-GGA	0.89
PWB6K	hybrid meta-GGA	0.90
MPWB1K	hybrid meta-GGA	0.91
PBE1KCIS	hybrid meta-GGA	0.93
MN12-SX	hybrid meta-NGA	0.93
mPWLYP	GGA	0.94
PW6B95	hybrid meta-GGA	0.95
M11-L	meta-GGA	0.99
MPW1B95	hybrid meta-GGA	1.02
B98	hybrid GGA	1.04
M06	hybrid meta-GGA	1.04
τHCTHhyb	hybrid meta-GGA	1.05
PBE1W	GGA	1.10
revTPSS	meta-GGA	1.11
PBELYP1W	GGA	1.11
MPW1K	hybrid GGA	1.12
LC-ωPBE	hybrid GGA	1.13
MPWLYP1W	GGA	1.16
MPW3PBE	hybrid GGA	1.18
B3LYP	hybrid GGA	1.20
B97-D3(BJ)	GGA/MM	1.22
TPSSLYP1W	meta-GGA	1.23
mPW1PW	hybrid GGA	1.26
MPWKCIS1K	hybrid meta-GGA	1.29
MPW1PBE	hybrid GGA	1.30
SCC-DFTB-γ^h	SCTB	1.31
N12	NGA	1.31
B97-3	hybrid GGA	1.33
TPSSh	hybrid meta-GGA	1.36
B97-D3	GGA/MM	1.38
TPSS	meta-GGA	1.39
PM6	NDDO	1.43
MN12-L	meta-NGA	1.45
B1B95	hybrid meta-GGA	1.57
BLYP	GGA	1.63
SCC-DFTB-γ^h-D(LJ)	SCTB/MM	1.73
B97−2	hybrid GGA	1.84
BB95	meta-GGA	1.91
SCC-DFTB	SCTB	2.02
PM3	NDDO	2.38
HCTH	GGA	2.39
revPBE	GGA	2.44
SCC-DFTB-D(LJ)	SCTB/MM	2.47
GKSVWN5	LSDA	2.69
O3LYP	hybrid GGA	3.16
PBEX	GGA	3.19
AM1-D	NDDO/MM	3.48
OLYP	GGA	3.83
RM1	NDDO	4.92
AM1	NDDO	5.55
OptX	GGA	6.62
MNDO	NDDO	13.64

[a]See the Results and Discussion section of the text for the definition of the characteristic error (CE).

"average" or "typical." Methods with a CE that is significantly less than 1.0 are considered "good," and these are the ones that we would recommend for use in simulations of water. Methods with a CE of close to or greater than 1.0 are not recommended as the first choices for use in simulations of water.

Using the CE values shown in Table 8 as the basis for our assessment, we find that the overall best methods for the calculation of binding and relative energies in various configurations of water molecules are ωB97X-D (CE = 0.10), LC-ωPBE-D3 (CE = 0.18), and M05-2X (CE = 0.23). These findings are consistent with Grimme's recent work[100] benchmarking DFT methods against a variety of noncovalent dimer interactions (including but not limited to water) and with our group's previous work benchmarking DFT methods against water hexamers:[15] Grimme recommends the LC-ωPBE-D3 method, and our previous study found M05-2X to be among the top methods for water energy calculations. Previous work by Grimme and co-workers[101] tested 47 density functionals against the GMTKN30 database for main group thermochemistry, kinetics, and noncovalent interactions and concluded that "[t]he most robust hybrid is Zhao and Truhlar's PW6B95 functional in combination with DFT-D3." We note that the PW6B95-D3 functional continues to do well in the present study with a CE of only 0.40.

Each of the methods singled out in the previous paragraph is a hybrid density functional, so it is also useful to name the functionals that do best without any Hartree−Fock exchange because those functionals can be employed with much less expense for extended systems—the best performing nonhybrid functionals are revPBE-D3 (CE = 0.55) and B97-D (CE = 0.68). These findings agree with Grimme's work,[101] where revPBE-D3

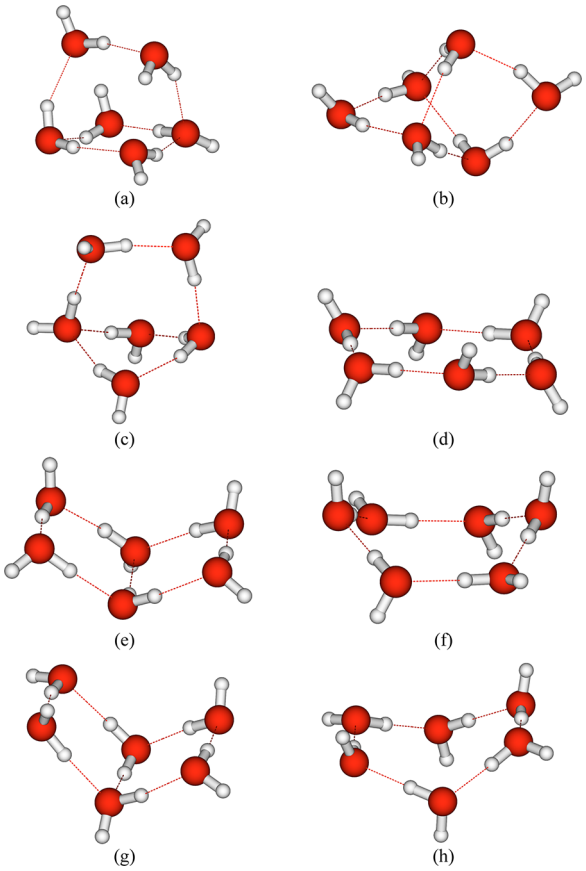

Figure 2. Water hexamers from ref 31. The structures are (a) prism, (b) cage, (c) bag, (d) cyclic-chair, (e) book-1, (f) cyclic-boat-1, (g) book-2, and (h) cyclic-boat-2.

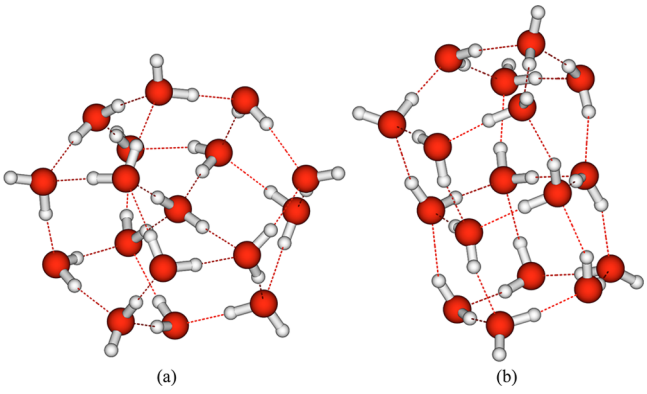

Figure 3. Water 17-mers from ref 32. The structures are (a) sphere and (b) 552′5.

and B97-D3 are recommended as the best nonhybrid functionals for main group thermochemistry, kinetics, and noncovalent interactions. The best nonhybrid without molecular mechanics terms in the present study is M06-L (CE = 0.70). We also note that N12-SX has a CE of only 0.43. Although N12-SX is nonlocal, it employs the screened exchange strategy developed by Scuseria and co-workers,[102] which means that it has no long-range nonlocality, and this makes it less expensive than other kinds of hybrid functionals for extended systems when certain computational algorithms are employed.

We find that two SWF methods actually have CE values that are equal to or lower than those of most nonhybrid density functionals; these methods are PMOv1 and PM3-D, having CE values of 0.50 and 0.58, respectively. The remaining SWF methods have CE values greater than 1.25.

As a final check to check whether the methods recommended for water in this study continue to do well on water nanoparticles and clusters of various sizes, we use the best DF, DF-MM, and SWF-MM methods for the water 16-mer binding energies to calculate the binding energies of the eight water hexamers from ref 31 and two water 17-mers from ref 32. These methods are M06-2X, ωB97X-D, and PM3-D, respectively. Because CAM-B3LYP and TPSSLYP are DF methods that performed well for the water 16-mer binding energies, we tested these methods on the water hexamers and water 17-mers also. The eight water hexamers are shown in Figure 2, and the two water 17-mers are shown in Figure 3. Ref 31 gives the CCSD(T)/CBS zero-point exclusive binding energies of the water hexamers, and ref 32 gives the CCSD(T)/aug-cc-pVTZ total electronic plus nuclear repulsion energies of the two water 17-mers. To calculate the binding energies of the water hexamers, the water monomer in its MP2/jul-cc-pVTZ optimized geometry was used, and for the binding energies of the water 17-mers, the water monomer in its MP2/aug-cc-pVTZ geometry was used (for consistency with the way in which the water 16-mer binding energies were calculated). The benchmark and DF, DF-MM, and SWF-MM binding energies of the water hexamers and water 17-mers are shown in Tables 9 and 10, respectively.

Tables 9 and 10 illustrate the importance of continuing to update our assessment of DF and SWF methods for water as high-level benchmark binding energies on larger water nanoparticles with new structural features become available. From Table 9, we see that the best methods for water 16-mer binding energies perform reasonably well for water hexamer binding energies, but they are not necessarily excellent. Table 10 shows, however, that the methods that did well for water 16-mers continue to perform well for water 17-mers, even though one of the 17-mers—the sphere—contains a structural feature not found in smaller nanoparticles: a truly interior four-coordinated

Table 9. Binding Energies (kcal/mol) of Water Hexamers and Mean Unsigned Errors (MUE, kcal/mol) in Density Functional and Semiempirical Calculations

method	prism	cage	bag	cyclic-chair	book-1	cyclic-boat-1	book-2	cyclic-boat-2	MUE
CCSD(T)/CBS	45.92	45.67	44.30	44.12	45.20	43.13	44.90	43.07	0.0
M06-L	49.50	49.04	46.52	45.24	47.11	44.29	46.88	44.20	2.1
TPSSLYP	47.65	47.91	47.85	48.86	48.95	47.76	48.63	47.63	3.6
ωB97X-D	49.79	49.73	48.14	47.89	49.06	46.87	48.79	46.80	3.8
M06-2X	51.67	51.05	48.42	47.87	49.30	46.77	48.93	46.74	4.3
CAM-B3LYP	49.59	49.72	49.02	50.06	50.25	48.88	49.83	48.81	5.0
PM3-D	50.62	53.28	51.18	51.85	53.33	50.88	53.19	51.20	7.4

dx.doi.org/10.1021/ct300848z | J. Chem. Theory Comput. 2013, 9, 995−1006

Table 10. Binding Energies (kcal/mol) of Water 17-mers and Mean Unsigned Errors (MUE, kcal/mol) in Density Functional and Semiempirical Calculations[a]

method	sphere	552′5	MUE(BE)	MUE(3)
CCSD(T)/aug-cc-pVTZ	182.54	181.84	0.0	0.0
M06-2X	182.25	179.51	1.3	1.6
CAM-B3LYP	179.17	180.47	2.4	2.2
ωB97X-D	180.02	178.91	2.7	2.0
PM3-D	188.50	182.33	3.2	4.0
TPSSLYP	177.31	179.98	3.5	3.5
M06-L	174.68	170.79	9.5	7.4

[a]MUE(BE) is the mean unsigned error in the two binding energies, and MUE(3) is the mean of three unsigned errors, in particular the two binding energies and the one relative energy.

water molecule that is surrounded by a roughly spherical solvation shell.

We will not summarize the rest of the findings in the tables line-by-line; the reader will probably find it easy enough to simply consult the tables for those functionals of particular interest.

4. CONCLUDING REMARKS

The absolute electronic plus nuclear repulsion energies of five $(H_2O)_{16}$ nanoparticles (also called water 16-mers) and two water 17-mers at the CCSD(T)/aug-cc-pVTZ level of theory are now available in the literature,[32] enabling the calculation of benchmark relative conformational energies and benchmark binding energies of these nanoparticles. Previously, the largest water particles for which such high-level *ab initio* energies were published were water hexamers. Water hexamers are excellent test cases for various types of electronic structure theory because they have stable low-energy two- and three-dimensional configurations lying within ∼1 kcal/mol of each other. However, water hexamers do not contain four-coordinated water molecules, i.e., water molecules that participate in four hydrogen bonds. The water 16-mers used in this study contain four-coordinated water molecules, making them an even more challenging and robust test case than the water hexamers. Two of the 16-mers (structures 4444-a and 4444-b) each contain eight four-coordinated water molecules and the remaining 16-mers (structures antiboat, boat-a, and boat-b) each contain four four-coordinated water molecules. Therefore, in the present study, we have used the binding and relative CCSD(T)/aug-cc-pVTZ energies of these five water 16-mers as benchmarks against which we have tested 12 SWF methods and 73 levels of DF theory.

For binding energies of water 16-mers, we find that the best method overall is the hybrid meta-GGA density functional M06-2X. The best nonhybrid density functional for water 16-mer binding energies is TPSSLYP, and the best semiempirical method is the dispersion-corrected SWF PM3-D. For relative energies of water 16-mers, we find that the best method overall is the hybrid GGA/MM functional ωB97X-D, closely followed by the hybrid GGA functional SOGGA11-X and the hybrid GGA/MM functional LC-ωPBE-D3. The best SWF method for relative energies of water 16-mers is PM6. Overall, taking both relative and binding energies into consideration, we find that the best functionals for water 16-mers are ωB97X-D, LC-ωPBE-D3 (with damping to zero), and M05-2X. The best SWF or SWF-MM methods for water 16-mers are PMOv1 and PM3-D, and the best nonhybrid functionals are revPBE-D3 and B97-D. The best nonhybrid without molecular mechanics for water 16-mers is M06-L. The best functional studied for water 17-mers is M06-2X.

■ ASSOCIATED CONTENT

Supporting Information

Tables giving all geometries used in this work, the M05-2X/jun-cc-pVTZ and LC-ωPBE-D3/jun-cc-pVTZ total energies in hartrees for each geometry, and the binding energies and characteristic errors of the water 16- and 17-mers based on the M06-L/aug-cc-pVTZ optimized water monomer geometry are available free of charge via the Internet at http://pubs.acs.org.

■ AUTHOR INFORMATION

Corresponding Author

*E-mail: truhlar@umn.edu.

Present Address

[†]Department of Chemistry, Wellesley College, 106 Central Street, Wellesley, MA 02481

Notes

The authors declare no competing financial interest.

■ ACKNOWLEDGMENTS

This work was supported in part by the National Science Foundation under grant no. CHE09-56776.

■ REFERENCES

(1) Wang, Y.; Babin, V.; Bowman, J. M.; Paesani, F. *J. Am. Chem. Soc.* **2012**, *134*, 11116.
(2) Cizek, J. *Adv. Chem. Phys.* **1969**, *14*, 35.
(3) Purvis, G. D.; Bartlett, R. J. *J. Chem. Phys.* **1982**, *76*, 1910.
(4) Raghavachari, K.; Trucks, G. W.; Pople, J. A.; Head-Gordon, M. *Chem. Phys. Lett.* **1989**, *157*, 479.
(5) Kohn, W. *Rev. Mod. Phys. Phys.* **2005**, *71*, 1253.
(6) Pople, J. A.; Beveridge, D. L. *Approximate Molecular Orbital Theory*; McGraw Hill: New York, 1970.
(7) Dahlke, E. E.; Truhlar, D. G. *J. Phys. Chem. B* **2005**, *109*, 15677.
(8) Oliveira, G. d.; Martin, J. M. L. J. *Chem. Phys.* **1999**, *111*, 1843.
(9) Parthiban, S.; Martin, J. M. L. J. *Chem. Phys.* **2001**, *114*, 6014.
(10) Zhao, Y.; Truhlar, D. G. *J. Phys. Chem. A* **2005**, *109*, 5656.
(11) Schmider, H. L.; Becke, A. D. *J. Chem. Phys.* **1998**, *108*, 9624.
(12) Zhao, Y.; Truhlar, D. G. *J. Phys. Chem. A* **2004**, *108*, 6908.
(13) Olson, R. M.; Bentz, J. L.; Kendall, R. A.; Schmidt, M. W.; Gordon, M. S. *J. Chem. Theory Comput.* **2007**, *3*, 1312.
(14) Papajak, E.; Truhlar, D. G. *J. Chem. Theory Comput.* **2011**, *7*, 10.
(15) Dahlke, E. E.; Olson, R. M.; Leverentz, H. R.; Truhlar, D. G. *J. Phys. Chem. A* **2008**, *112*, 3976.
(16) Møller, C.; Plesset, M. S. *Phys. Rev.* **1934**, *46*, 618.
(17) Woon, D. E.; Dunning, T. H., Jr. *J. Chem. Phys.* **1993**, *98*, 1358.
(18) Woon, D. E.; Dunning, T. H., Jr. *J. Chem. Phys.* **1994**, *100*, 2975.
(19) Wilson, A. K.; Woon, D. E.; Peterson, K. A.; Dunning, T. H., Jr. *J. Chem. Phys.* **1999**, *110*, 7667.
(20) Koput, J.; Peterson, K. A. *J. Phys. Chem. A* **2002**, *106*, 9595.
(21) Balabanov, N. B.; Peterson, K. A. *J. Chem. Phys.* **2005**, *123*, 064107.
(22) Dunning, T. H., Jr. *J. Chem. Phys.* **1989**, *90*, 1007.
(23) Kendall, R. A.; Dunning, T. H., Jr.; Harrison, R. J. *J. Chem. Phys.* **1992**, *96*, 6796.
(24) Zhao, Y.; Schultz, N. E.; Truhlar, D. G. *J. Chem. Theory Comput.* **2006**, *2*, 364.
(25) Perdew, J. P.; Burke, K.; Ernzerhof, M. *Phys. Rev. Lett.* **1996**, *77*, 3865.
(26) Adamo, C.; Barone, V. *J. Chem. Phys.* **1999**, *110*, 6158.
(27) Nachimuthu, S.; Gao, J.; Truhlar, D. G. *Chem. Phys.* **2012**, *400*, 8.
(28) Zhao, Y.; Truhlar, D. G. *Theor. Chem. Acc.* **2008**, *120*, 215.

(29) Elstner, M.; Porezag, G.; Jungnickel, G.; Elsner, M.; Haugk, M.; Frauenheim, T.; Suhai, S.; Seifert, G. *Phys. Rev. B* **1998**, *58*, 7260.
(30) Zhang, P.; Fiedler, L.; Leverentz, H. R.; Truhlar, D. G.; Gao, J. *J. Chem. Theory Comput.* **2011**, *7*, 857.
(31) Bates, D. M.; Tschumper, G. S. *J. Phys. Chem. A* **2009**, *113*, 3555.
(32) Yoo, S.; Aprà, E.; Zeng, X. C.; Xantheas, S. S. *J. Phys. Chem. Lett.* **2010**, *1*, 3122.
(33) Becke, A. D. *Phys. Rev. A* **1988**, *38*, 3098.
(34) Becke, A. D. *J. Chem. Phys.* **1996**, *104*, 1040.
(35) Lee, C.; Yang, W.; Parr, R. G. *Phys. Rev. B* **1988**, *37*, 785.
(36) Boese, A. D.; Martin, J. M. L. *J. Chem. Phys.* **2004**, *121*, 3405.
(37) Stephens, P. J.; Devlin, F. J.; Chabalowski, C. F.; Frisch, M. J. *J. Phys. Chem.* **1994**, *98*, 11623.
(38) Hamprecht, F. A.; Cohen, A. J.; Tozer, D. J.; Handy, N. C. *J. Chem. Phys.* **1998**, *109*, 6264.
(39) Wilson, P. J.; Bradley, T. J.; Tozer, D. J. *J. Chem. Phys.* **2001**, *115*, 9233.
(40) Keal, T. W.; Tozer, D. J. *J. Chem. Phys.* **2005**, *123*, 121103.
(41) Grimme, S. *J. Comput. Chem.* **2006**, *27*, 1787.
(42) Grimme, S.; Antony, J.; Ehrlich, S.; Krieg, H. *J. Chem. Phys.* **2010**, *132*, 154104.
(43) Becke, A. D.; Johnson, E. R. *J. Chem. Phys.* **2005**, *122*, 154101.
(44) Johnson, E. R.; Becke, A. D. *J. Chem. Phys.* **2005**, *123*, 024101.
(45) Johnson, E. R.; Becke, A. D. *J. Chem. Phys.* **2006**, *124*, 174104.
(46) Yanai, T.; Tew, D.; Handy, N. *Chem. Phys. Lett.* **2004**, *393*, 51.
(47) Kohn, W.; Sham, L. J. *Phys. Rev.* **1965**, *140*, A1133.
(48) Vosko, S. H.; Wilk, L.; Nusair, M. *Can. J. Phys.* **1980**, *58*, 1200.
(49) Krukau, A. V.; Vydrov, O. A.; Izmaylov, A. F.; Scuseria, G. E. *J. Chem. Phys.* **2006**, *125*, 224106.
(50) Vydrov, O. A.; Scuseria, G. E.; Perdew, J. P. *J. Chem. Phys.* **2007**, *126*, 154109.
(51) Peverati, R.; Truhlar, D. G. *Phys. Chem. Chem. Phys.* **2012**, *14*, 13171.
(52) Peverati, R.; Truhlar, D. G. *Phys. Chem. Chem. Phys.* Online as Accepted Article. DOI: 10.1039/C2CP42576A.
(53) Adamo, C.; Barone, V. *J. Chem. Phys.* **1998**, *108*, 664.
(54) Perdew, J. P. In *Electronic Structure of Solids '91*; Ziesche, P., Eschig, H., Eds.; Akademie Verlag: Berlin, 1991; p 11.
(55) Lynch, B. J.; Fast, P. L.; Harris, M.; Truhlar, D. G. *J. Phys. Chem. A* **2000**, *104*, 4811.
(56) Zhao, Y.; González-García, N.; Truhlar, D. G. *J. Phys. Chem. A* **2005**, *109*, 2012.
(57) Zhao, Y.; Schultz, N. E.; Truhlar, D. G. *J. Chem. Phys.* **2005**, *123*, 161103.
(58) Zhao, Y.; Truhlar, D. G. *J. Chem. Phys.* **2006**, *125*, 194101.
(59) Zhao, Y.; Truhlar, D. G. *J. Chem. Theory Comput.* **2008**, *4*, 1849.
(60) Peverati, R.; Truhlar, D. G. *J. Phys. Chem. Lett.* **2011**, *2*, 2810.
(61) Peverati, R.; Truhlar, D. G. J. *Phys. Chem. Lett.* **2012**, *3*, 117.
(62) Peverati, R.; Truhlar, D. G. *J. Chem. Theory Comput.* **2012**, *8*, 2310.
(63) Handy, N. C.; Cohen, A. J. *Mol. Phys.* **2001**, *99*, 403.
(64) Hoe, W.-M.; Cohen, A. J.; Handy, N. C. *Chem. Phys. Lett.* **2001**, *341*, 319.
(65) Cohen, A. J.; Handy, N. C. *Mol. Phys.* **2001**, *99*, 607.
(66) Zhao, Y.; Truhlar, D. G. *J. Chem. Theory Comput.* **2005**, *1*, 415.
(67) Rey, J.; Savin, A. *Int. J. Quantum Chem.* **1998**, *69*, 581.
(68) Kreiger, J. B.; Chen, J.; Iafrate, G. J.; Savin, A. In *Electronic Correlations and Materials Properties*; Gonis, A., Kioussis, N., Eds; Plenum: New York, 1999; p 463.
(69) Toulouse, J.; Savin, A.; Adamo, C. *J. Chem. Phys.* **2002**, *117*, 10465.
(70) Zhang, Y.; Yang, W. *Phys. Rev. Lett.* **1997**, *80*, 890.
(71) Perdew, J. P.; Ruzsinszky, A.; Csonka, G. I.; Constantin, L. A.; Sun. *J. Phys. Rev. Lett.* **2009**, *103*, 026403.
(72) Peverati, R.; Truhlar, D. G. *J. Chem. Phys.* **2011**, *135*, 191102.
(73) Tao, J.; Perdew, J. P.; Staroverov, V. N.; Scuseria, G. E. *Phys. Rev. Lett.* **2003**, *91*, 146401−1.
(74) Perdew, J. P.; Tao, J.; Staroverov, V. N.; Scuseria, G. E. *J. Chem. Phys.* **2004**, *120*, 6898.
(75) Staroverov, V. N.; Scuseria, G. E.; Tao, J.; Perdew, J. P. *J. Chem. Phys.* **2003**, *119*, 12129.
(76) Xu, X.; Goddard, W. A., III. *Proc. Natl. Acad. Sci. U. S. A.* **2004**, *101*, 2673.
(77) Boese, A. D.; Handy, N. C. *J. Chem. Phys.* **2002**, *116*, 9559.
(78) Chai, J.-D.; Head-Gordon, M. *J. Chem. Phys.* **2008**, *128*, 084106.
(79) Chai, J.-D.; Head-Gordon, M. *Phys. Chem. Chem. Phys.* **2008**, *10*, 6615.
(80) Dewar, M. J. S.; Zoebisch, E. G.; Healy, E. F.; Stewart, J. J. P. *J. Am. Chem. Soc.* **1985**, *107*, 3902.
(81) McNamara, J. P.; Hillier, I. H. *Phys. Chem. Chem. Phys.* **2007**, *9*, 2362.
(82) Morgado, C. A.; McNamara, J. P.; Hillier, I. H.; Burton, N. A.; Vincent, M. A. *J. Chem. Theory Comput.* **2007**, *3*, 1656.
(83) Dewar, M. J. S.; Thiel, W. *J. Am. Chem. Soc.* **1977**, *99*, 4899.
(84) Stewart, J. J. P. *J. Comput. Chem.* **1989**, *10*, 209.
(85) Stewart, J. J. P. *J. Mol. Model.* **2007**, *13*, 1173.
(86) Rocha, G. B.; Freire, R. O.; Simas, A. M.; Stewart, J. J. P. *J. Comput. Chem.* **2006**, *27*, 1101.
(87) Yang, Y.; Yu, H.; York, D.; Cui, Q.; Elstner, M. *J. Phys. Chem. A* **2007**, *111*, 10861.
(88) Zhechkov, L.; Heine, Th.; Patchkovskii, S.; Seifert, G.; Duarte, H. A. *J. Chem. Theory Comput.* **2005**, *1*, 841.
(89) Stewart, J. J. P.; Fiedler, L. J.; Zhang, P.; Zheng, J.; Rossi, I.; Hu, W.-P.; Lynch, G. C.; Liu, Y.-P.; Chuang, Y.-Y.; Pu, J.; Li, J.; Cramer, C. J.; Fast, P. L.; Gao, J.; Truhlar, D. G. *MOPAC*, version 5.018mn; University of Minnesota: Minneapolis, MN.
(90) Zhao, Y.; Peverati, R.; Yang, K.; Truhlar, D. G. *Minnesota Gaussian Functional Module (MN-GFM)*, version 6.4; University of Minnesota: Minneapolis, MN, 2012.
(91) Frisch, M. J.; Trucks, G. W.; Schlegel, H. B.; Scuseria, G. E.; Robb, M. A.; Cheeseman, J. R.; Scalmani, G.; Barone, V.; Mennucci, B.; Petersson, G. A.; Nakatsuji, H.; Caricato, M.; Li, X.; Hratchian, H. P.; Izmaylov, A. F.; Bloino, J.; Zheng, G.; Sonnenberg, J. L.; Hada, M.; Ehara, M.; Toyota, K.; Fukuda, R.; Hasegawa, J.; Ishida, M.; Nakajima, T.; Honda, Y.; Kitao, O.; Nakai, H.; Vreven, T.; Montgomery, J. A., Jr.; Peralta, J. E.; Ogliaro, F.; Bearpark, M.; Heyd, J. J.; Brothers, E.; Kudin, K. N.; Staroverov, V. N.; Kobayashi, R.; Normand, J.; Raghavachari, K.; Rendell, A.; Burant, J. C.; Iyengar, S. S.; Tomasi, J.; Cossi, M.; Rega, N.; Millam, J. M.; Klene, M.; Knox, J. E.; Cross, J. B.; Bakken, V.; Adamo, C.; Jaramillo, J.; Gomperts, R.; Stratmann, R. E.; Yazyev, O.; Austin, A. J.; Cammi, R.; Pomelli, C.; Ochterski, J. W.; Martin, R. L.; Morokuma, K.; Zakrzewski, V. G.; Voth, G. A.; Salvador, P.; Dannenberg, J. J.; Dapprich, S.; Daniels, A. D.; Farkas, Ö.; Foresman, J. B.; Ortiz, J. V.; Cioslowski, J.; Fox, D. J. *Gaussian 09*, Revision C.1; Gaussian, Inc.: Wallingford, CT, 2009.
(92) Wilhelms, W.; Grimme, S.; Antony, J.; Ehrlich, S.; Krieg, H. *DFT-D3*, version 2.1, revision 3; Universität Münster: Münster, Germany, 2011. http://toc.uni-muenster.de/DFTD3/index.html (accessed Aug 2012.)
(93) Aradi, B.; Hourahine, B.; Frauenheim, Th. *J. Phys. Chem. A* **2007**, *111*, 5678.
(94) Elstner, M. Ph.D. Dissertation, Universitaet Paderborn, Paderborn, Germany, 1998. (See also http://www.dftb.org/parameters/download/.)
(95) Slater, J. C.; Koster, G. F. *Phys. Rev.* **1954**, *94*, 1498.
(96) Fischer-Hjalmars, I. *J. Chem. Phys.* **1965**, *42*, 1962.
(97) Vela, A.; Gázquez, J. L. *J. Phys. Chem.* **1988**, *92*, 5688.
(98) Goyal, P.; Elstner, M.; Cui, Q. *J. Phys. Chem. B* **2011**, *115*, 6790.
(99) Rappe, A. K.; Casewit, C. J.; Colwell, K. S.; Goddard, W. A., III; Skiff, W. M. *J. Am. Chem. Soc.* **1992**, *114*, 10024.
(100) Goerigk, L.; Kruse, H.; Grimme, S. *Chem. Phys. Chem.* **2011**, *12*, 3421.
(101) Goerigk, L.; Grimme, S. *Phys. Chem. Chem. Phys.* **2011**, *13*, 6670.
(102) Heyd, J.; Scuseria, G. E.; Ernzerhof, M. *J. Chem. Phys.* **2003**, *118*, 8207.